INSTITUTE OF PHYSICS PUBLISHING MEASUREMENT SCIENCE AND TECHNOLOGY

Meas. Sci. Technol. **13** (2002) 1482–1487 PII: S0957-0233(02)37807-X

Design and characterization of an atomic beam oven for combined laser and electron impact experiments

Danica Cvejanovic and Andrew James Murray

Department of Physics and Astronomy, The University of Manchester, Manchester M13 9PL, UK

E-mail: Danica@fs3.ph.man.ac.uk and Andrew.Murray@man.ac.uk

Received 7 June 2002, accepted for publication 3 July 2002
Published 14 August 2002
Online at stacks.iop.org/MST/13/1482

Abstract

As both experimental and theoretical studies in atomic physics move towards more complex atoms and more sophisticated methods, the design and characterization of atomic beam sources is becoming important as specific requirements emerge. This is especially the case when both electron impact and laser excitation are combined. The design of an oven is presented here together with characterization of the atomic beam parameters of importance to both electron impact and laser excitation experiments. The oven is designed and tested using calcium but is relevant for a range of atoms. In this study the oven was tested at temperatures up to 710 °C.

Keywords: atomic beams, atomic ovens, calcium beams

M This article features online multimedia enhancements

1. Introduction

A review of atomic beam ovens covering available information for a large number of atomic species has been published recently by Ross and Sontag [1]. The review includes a substantial amount of practical design information and gives a good reference background. Another aspect important in oven design, i.e. spatial profiles of effusive atomic beams, has been most recently studied by Buckman *et al* [2] for a number of species which are in the gas phase at room temperature. These authors give a good overview of earlier references relating to atomic beam properties. Both design characteristics of the ovens and properties of the effusive beams discussed in the above-mentioned papers and references therein are nowadays increasingly important for experiments other than electron scattering. Studies involving synchrotron radiation or laser excitation of atoms are two examples, and such experiments have additional specific requirements.

In this paper the design of an oven for calcium is reported which requires reasonably high temperature to satisfy intensity requirements having in mind both electron scattering and laser excitation experiments. Using a tunable CW laser, fluorescence from laser-excited atoms has been used to characterize aspects of the atomic beam which are of interest to both electron scattering and laser excitation experiments. Parameters which have been determined include the Doppler profile of the beam, the total fluorescence intensity, which is proportional to the number of atoms in the beam, and the polarization of the emitted fluorescence, which indicates resonance trapping. These parameters were measured as a function of temperature which can be directly related to the driving pressure. Information from such a study is in some aspects complementary to previous studies [2, 3] and is of practical interest for different experiments.

Previous studies on calcium atoms include electron impact experiments [4–8], combined laser excitation and electron impact experiments [9], a number of photoionization experiments using synchrotron radiation [10–15] and studies using pulsed laser photoionization of oriented calcium [16]. These experiments used different types of atomic ovens but to the best of our knowledge no detailed characterization of atomic beams has been published. General considerations and requirements in the superelastic electron scattering experiments of Law and Teubner [9] are the nearest to the present experiments. In addition, the laser cooling of calcium [17, 18] is closely related to the present work.

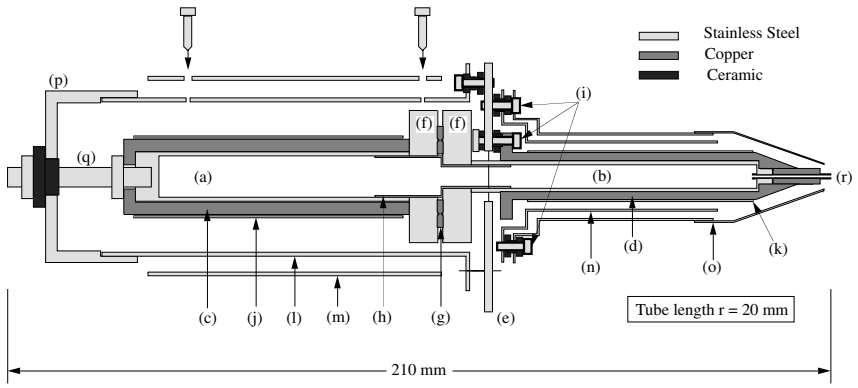

Figure 1. Scaled diagram of the oven: (a) body; (b) nozzle; (c) body heater; (d) nozzle heater; (e) oven holding and centring plate; (f) flanges; (g) copper gasket; (h) protective sleeve for copper gasket; (i) ceramic insulated stainless steel screws; (j, k) heating coils cover; (l) inner and (m) outer shield on body; (n) inner and (o) outer shield on nozzle; (p) end-cup locked onto the inner body shield; (q) Macor insulated M5 stud.

Design criteria of the present oven are based on requirements imposed by a relatively complex experiment utilizing laser excitation of calcium followed by electron impact ionization. The coherent nature of the laser excitation results in specific preparation of excited targets and a coincidence based (e,2e) study in an electron spectrometer will then be used to investigate fine details of the ionization of optically prepared, aligned and oriented atoms. Hence in the present oven design, both the laser excitation process and the design of the existing electron spectrometer were considered. These design criteria can be divided into two groups. The first group relates directly to the principle of the experiment and includes the following:

(1) The alignment and orientation of atoms excited by the laser radiation must be preserved, so radiation trapping in the atomic beam has to negligible.
(2) The Doppler profile of the atomic beam and its associated detuning from line resonance has to be optimized for efficient optical pumping.

Taking into account (1) and (2), the aim is to produce the highest possible excited-atom density to improve data collection efficiency.

The second set of criteria are common to all electron impact experiments and are of purely practical importance, but they do indirectly influence the performance of the experiment. These criteria include the efficient use of sample material and low contamination of the electron impact spectrometer to ensure stable operation over long periods of time.

Some of the constraints on the present design were set by the existing (e,2e) experiment where this oven is to be located [19], but most were based on criteria valid generally. Testing and characterization of the oven was implemented in a dedicated vacuum chamber and the results are presented here along with details of the design. In addition, a number of solutions to problems encountered in this design are discussed.

2. Design criteria and implementation

A scaled diagram of the oven is shown in figure 1. This diagram, as well as a detailed set of CAD drawings, can be found in the file OVENCAD.pdf on the web link associated with this paper.

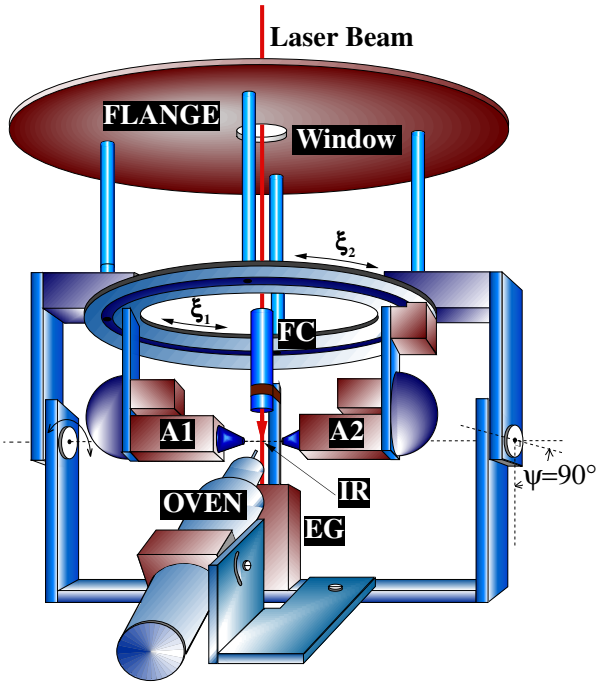

Figure 2. The (e,2e) experiment at Manchester incorporating the calcium oven. The spectrometer is shown in the perpendicular plane ($\psi = 90°$) where the electron gun (EG) is perpendicular to the detection plane defined by analysers A1 and A2 which rotate through angles ξ_1 and ξ_2. The interaction region (IR) is defined by the electron beam and atomic beam. Unscattered electrons are collected in the Faraday cup (FC). The laser beam enters the chamber through an optical window located in the top flange.

The main feature of this design is that the body (a) and nozzle (b), where the calcium sample is vaporized, are separate from the heaters (c) and (d). This permits precise positioning of the effusing atomic beam with respect to the electron beam and detectors, allowing the interaction region in the (e,2e) spectrometer to be well defined, as shown in figure 2. This is achieved by fixed positioning of the nozzle heater (d) into which the oven slides, onto a 2 mm thick stainless steel plate (e), which acts as the main support for the oven. The nature of this design makes this oven particularly easy to use, since

all components apart from the body (a) and nozzle (b) are permanently secured inside the vacuum system. Refilling the oven requires the simple task of extracting the body and nozzle, refilling, securing a new gasket (g) and re-inserting into the oven assembly without loss of alignment.

Calcium is loaded into the body (a), while the atomic beam effuses through a 20 mm long exit tube (r) which has inner diameter of 0.9 mm, fitted into the nozzle (b). Two 34 mm diameter conflat flanges (f) couple the two sections of the oven together, a copper gasket (g) providing the seal. Over a period of several months of operation it was discovered that the hot calcium vapour reacted with this gasket, destroying the copper seal and allowing the oven to leak. To eliminate this problem a stainless steel sleeve (h) was hence retrofitted between the body (a) and nozzle (b).

Transfer of heat from the nozzle heater to the oven mount is minimized by utilizing three-point fixing using stainless steel M2 screws (i) insulated by ceramics. This method of fixing is adopted for other parts of the oven including the mounting of the complete assembly onto the base plate. This provides low heat loss and reduces heating of surrounding parts inside the vacuum chamber. After several days of continuous operation at 700 °C, the temperature on the base below the oven, and on all other parts of the chamber, never exceeded 45 °C.

Two separate heaters, (c) for the body and (d) for the nozzle, provide a variable temperature differential of up to 100 °C between the body and nozzle. The heaters are made with bi-filar heating coils incorporating cold ends, so that minimal magnetic fields are generated by the heating currents. The heating coils are custom made by Thermocoax [20] and are wound in helical grooves onto heaters (c) and (d) (not shown in figure 1). Heater bodies (c) and (d) are manufactured from oxygen-free copper. This choice of heater coil with integral cold ends makes wiring of the oven easy and the heaters are found to be robust. Copper is used for the heater bodies since this provides good heat transfer to the inner part of the oven and the exit tube. Stainless steel sleeves (j) and (k) surround the coils, ensuring good thermal contact with the copper. These sleeves additionally act as radiation shields. The temperature of the oven is monitored using two commercial K-type thermocouples, again custom made by Thermocoax. These thermocouples are of the same design and diameter as the heaters and are located in helical grooves near the exit of the beam and at the base of the oven.

Radiation losses from the oven resulting in undesired heating of nearby components is reduced by 316 grade stainless steel radiation shields. Two shields (l) and (m) are located at the body, and two shields (n) and (o) are located at the nozzle. The shields are permanently attached to each other and to the stainless steel plate (e), allowing body and nozzle to be detached for refilling or maintenance. The body and nozzle are fixed onto the oven mount via the inner body shield (l) using an end cup (p) and Macor-insulated M5 stud (q).

Custom-built constant-current power supplies were used to drive the heaters to achieve stable temperature within 1 °C over long periods of time. The heaters each have a resistance of 65 Ω when cold and currents up to 0.7 A were required to achieve temperatures of 700 °C for the nozzle and 670 °C for the body. At these temperatures the nozzle was observed to be red hot when viewed through an optical window.

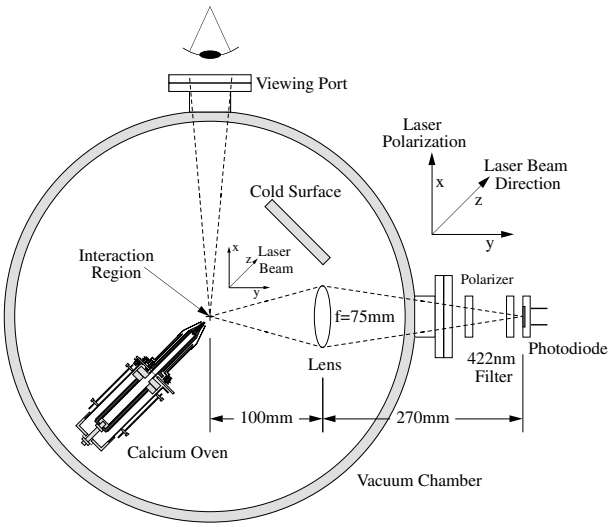

Figure 3. Schematic diagram of the experiment in the test chamber, showing the position of the oven, fluorescence collection optics and cold surface for deposition of the atomic beam.

Two points of interest are worth mentioning. The calcium load was always handled in an argon atmosphere as suggested by Ross [21]. Similarly, the vacuum chamber was filled with argon prior to opening to air and the exit tube of the oven was blocked to prevent oxidation of the calcium sample once open.

A flat circular copper disc cooled by a constant flow of water intercepted the atomic beam at a distance of 50 mm from the exit of the oven as shown in figure 3. Calcium which condensed on this cold surface made a clearly identifiable circle of diameter ∼5 mm, allowing the atom beam divergence angle to be estimated to be around 3°. Under normal operation the quantity of calcium which condensed elsewhere in the vacuum chamber was negligible. It was only when the copper gasket (g) was destroyed (as noted above) that significant contamination of surrounding surfaces was observed. Even at this time, the contamination was mostly confined to shields (j) and (k) and holding plate (p).

Figure 2 shows the (e,2e) experiment where the oven is to be used for ionization experiments from laser-excited calcium. The position of the oven relative to the electron gun (EG), Faraday cup (FC) and electron analysers (A1) and (A2) can be seen. The electron analysers rotate in the horizontal plane and define the detection plane whereas the electron gun can rotate from a position perpendicular to the detection plane (as shown in the figure) through to a position within the detection plane. The oven and Faraday cup are to be located on the same assembly as the gun and will rotate with the gun. Laser radiation is incident perpendicular to the detection plane through a window located on the top flange. As can be seen, the available space imposes exacting constraints on the design of the oven.

3. Results and discussion

The functioning of the oven and the properties of the calcium beam have been investigated by monitoring fluorescence emitted from calcium atoms excited by resonant laser excitation. The Doppler profile of the atomic beam, intensity of fluorescence and polarization of the emitted radiation were all

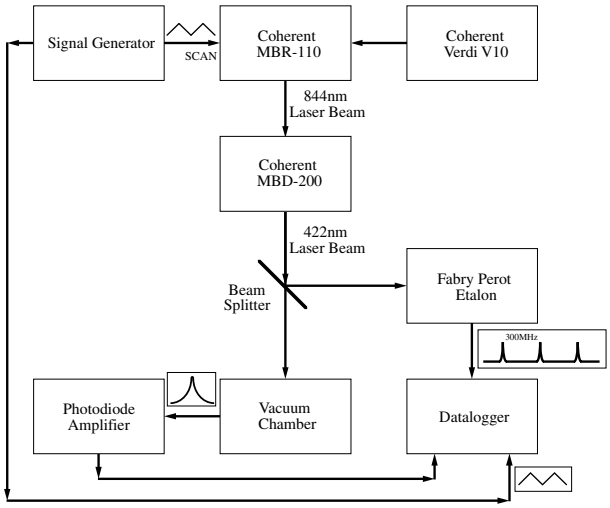

Figure 4. Block diagram showing the data collection electronics. The laser frequency is controlled by the signal generator and is monitored by the 300 MHz Fabry–Perot etalon. The fluorescence, etalon peaks and signal generator output are logged by a Pico Technologies datalogger.

measured for a range of oven temperatures and as a function of laser intensity. These properties are of interest both for optical pumping and electron impact experiments since they give an accurate representation of the characteristics of the atomic beam.

3.1. The experimental arrangement

To evaluate the properties of the calcium oven a test chamber was setup as shown in figure 3. Resonant laser radiation is provided by a Coherent MBR-110 Ti:sapphire laser and a Coherent MBD-200 frequency doubler. The MBR-110 laser is pumped by a Coherent Verdi-V10 laser. This system provides up to 150 mW of laser radiation at 422 nm with a polarization purity in excess of 500:1. Laser light with polarization vector along the vertical direction (x axis in figure 3) is incident perpendicular to the axis of the atomic beam oven and is focused to a beam waist of approximately 1 mm at the interaction region located 5 mm from the exit tube of the oven. Calcium atoms are excited by laser radiation from the $(4s)^2\,{}^1S$ ground state to the first excited $(4s4p)\,{}^1P$ state and fluorescence emitted perpendicular to the laser beam is detected.

The vertical plane through the interaction region shown in figure 3 contains the axis of the atomic beam and the axis of the optical system used for analysis and detection of fluorescence. The oven is positioned at 45° to the horizontal yz-plane. The fluorescence detection system consists of a 50 mm diameter lens of focal length 75 mm located inside the vacuum chamber which images the interaction region onto a photodiode (PD) detector located outside the chamber. The magnification of this optical system is $M = 2.6$. Resonance fluorescence from laser excitation at 422.6703 nm (measured using a Burleigh WA-1500 wavemeter) is selected using an interference filter with a transmission width of 7 nm. Polarization analysis of the fluorescence is performed by insertion of a dichroic polarizer prior to the detector. A second optical window positioned perpendicular to the horizontal plane permits visual observation of the fluorescence.

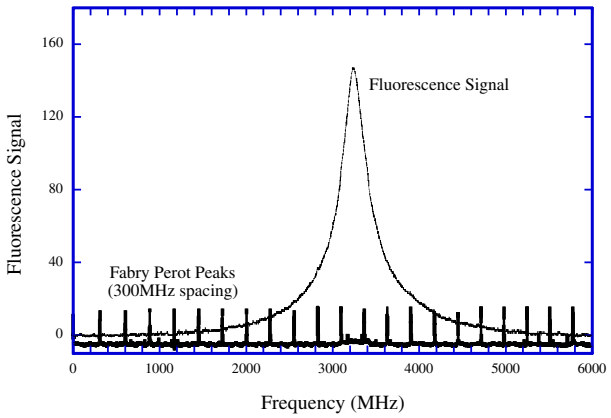

Figure 5. Doppler profile measured at a temperature of $T = 530\,°C$. Fabry–Perot signals with peaks at a separation of 300 MHz used for calibration of the frequency scale are also shown for reference.

Two PD detectors were used to detect the fluorescence. The first was a Centronic OSD15-5T PD with an active area of 3.8 mm × 3.8 mm. Hence an interaction region of diameter ∼1.5 mm was imaged by the lens onto this detector. The observed interaction volume was decreased in some experiments to ∼0.3 mm by insertion of a 1 mm diameter aperture in front of the PD. A second Centronic QD50-5T PD with a circular detection area of diameter 7.8 mm was also used to measure fluorescence from a larger volume of diameter ∼3 mm.

A linear ramp from a Thurlby Thandar Instruments TGA-1241 arbitrary waveform generator was used to scan the laser frequency. The frequency axis was calibrated using a Coherent Fabry–Perot interferometer which has a free spectral range of 300 MHz. Part of the laser beam was fed to the interferometer and the output was detected simultaneously with the fluorescence signal. Fringes from the interferometer were used to calibrate the frequency scale for each scan. The PD intensity, voltage controlling the laser and output from the Fabry–Perot interferometer were logged into a personal computer using a Pico Technology data logger as shown in figure 4.

3.2. Measurement of the fluorescence profile

The Doppler profile of the atomic beam is principally influenced by two factors: the Maxwellian distribution of individual atomic velocities and the angular spread of the effusing beam, i.e. the direction at which individual atoms emerge. The angular spread of the atomic beam depends on the geometry of the exit tube and the type of flow from the oven. Different conditions and hence characteristics of the beam have been discussed in detail by Giordmaine and Wang [3]. For a given exit nozzle geometry, the angular spread evolves from one characterizing a well defined atomic beam at low temperature and low values of driving pressure to one approximating a cosine pattern at higher driving pressures where viscous flow dominates.

A precise quantitative description has been obtained by measuring the fluorescence profile as described above for a range of body and nozzle temperatures. A representative profile is shown in figure 5 for a body temperature $T_B = 530\,°C$ and for a 1 mm aperture in front of the PD. Fringes from the Fabry–Perot interferometer used for calibration of the frequency axis are also shown. In most of these measurements

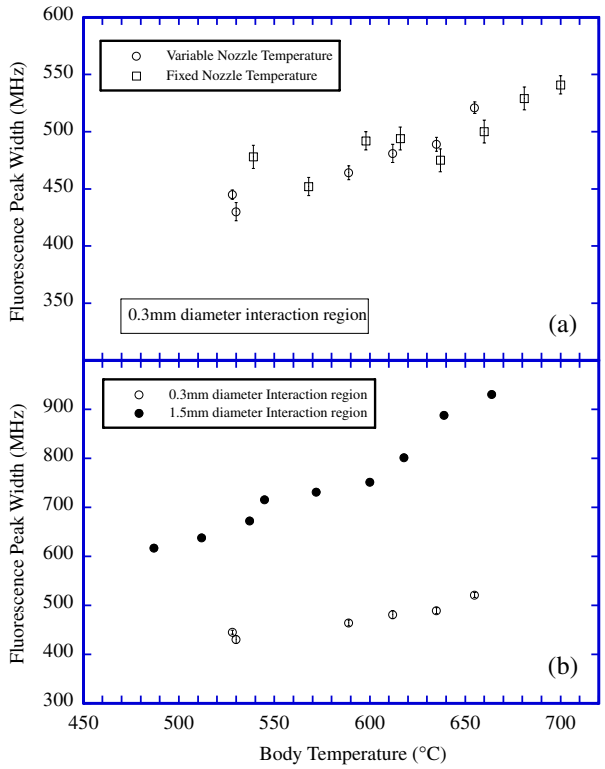

Figure 6. (a) Measured Doppler width as a function of body temperature. Open circles: both body and nozzle temperature are varied; open squares: nozzle is kept at a constant temperature of 710 °C. Fluorescence is detected from an interaction region of diameter 0.3 mm. (b) Both body and nozzle temperature are varied and fluorescence is detected from interaction regions of different size. Open circle: interaction volume of diameter 0.3 mm. Full circle: interaction volume of diameter 1.5 mm.

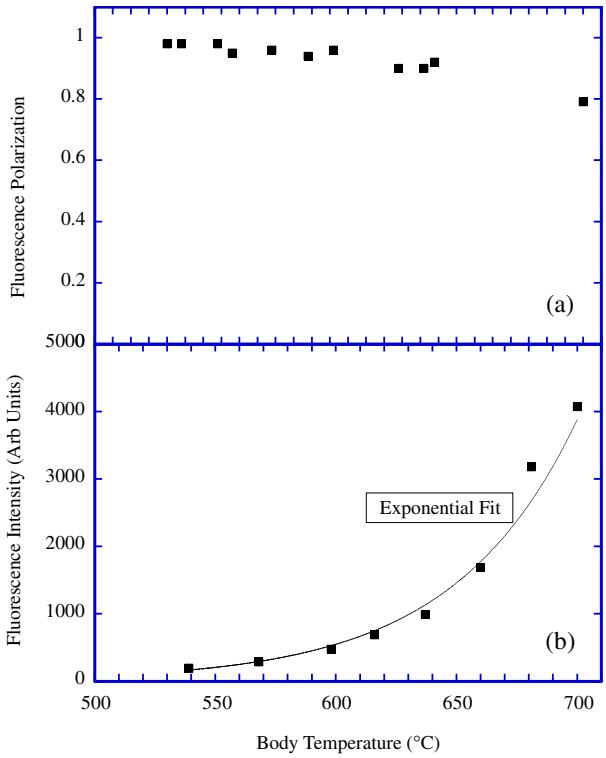

Figure 7. Polarization (a) and intensity (b) of the emitted fluorescence as a function of oven temperature. Significant depolarization occurs at temperatures in excess of 650 °C. The intensity and hence atomic beam density in the interaction region are seen to increase exponentially with temperature.

several sets of data were obtained and the values in the following graphs represent the weighted mean of these results.

The intensity profiles were measured for different operating modes of the oven and for different interaction volumes from which fluorescence was detected. Dependence of the width of the profile on oven temperature is shown in figure 6. Data shown in figure 6(a) have been obtained from an interaction volume of diameter ∼0.3 mm. The first set of data represented by open circles was obtained by varying the temperature of the body and nozzle simultaneously, maintaining a temperature difference of around 40 °C with the nozzle being hotter. To further investigate the influence which the nozzle temperature may have on the fluorescence profile, a set of measurements was also conducted with a constant nozzle temperature of 710 °C as the body temperature was adjusted. These data are shown as open squares. As can be seen from figure 6(a), the temperature of the nozzle does not have any significant effect on the width of the fluorescence profile.

By contrast, figure 6(b) shows the width of the intensity profile obtained by detecting fluorescence from interaction regions of different size. In this figure open circles represent the width obtained with an interaction region of diameter ∼0.3 mm, whereas the full circles correspond to fluorescence from a region of diameter ∼1.5 mm. In the second case, fluorescence from atoms with larger off-axis trajectories is also detected, resulting in a significant increase in the width of the measured profile.

3.3. Measurement of the polarization of the emitted fluorescence

Excitation of calcium atoms by linearly polarized laser radiation results in a very precise population of magnetic sublevels of the excited target. As a result, the fluorescence emitted at right angles to the experimental geometry as depicted in figure 3 should be 100% polarized, assuming that the laser radiation is fully polarized and that there are no processes leading to depolarization. The polarization of the laser radiation is improved using a Glan-Laser polarizer to achieve linear polarization of 99.99% or better. Resonance trapping of radiation in the atomic beam can, however, lead to significant depolarization of the detected fluorescence. Radiation trapping depends on the atomic beam density, and a study of the polarization of the fluorescence as a function of oven temperature (and hence beam density) allows an upper temperature to be determined where resonance trapping becomes significant.

Figure 7(a) shows the result of these studies, where the polarization of the radiation is plotted as a function of body temperature. By contrast, figure 7(b) shows the intensity of the fluorescence, which corresponds to the number density of excited targets in the beam. These results clearly illustrate the conflicting requirements of achieving a high number density with the requirement to minimize radiation trapping. The beam density is seen to increase exponentially with increasing temperature, however at temperatures above 650 °C, depolarization due to radiation trapping increases to

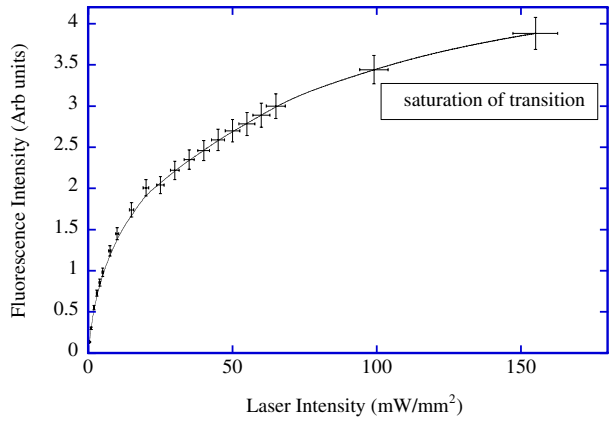

Figure 8. Variation of fluorescence intensity (and hence number density of excited atoms) as a function of the intensity of the laser radiation driving the transition.

more than 5%, which is unacceptable in many experiments. In this case it is necessary to operate the oven at temperatures below 650 °C, where the beam density is almost four times lower than at a temperature of 700 °C.

For these measurements a Newport dichroic sheet polarizer (part number 10LP-VIS) was used. The extinction ratio of this polarizer was determined experimentally to be in excess of 200:1, yielding a polarization efficiency of 99.5%. As a further check on the effects of optical pumping by the laser, the polarization of the emitted fluorescence was also measured as a function of incident laser intensity from 1 to 150 mW mm^{-2}. No change of polarization was detected for this range of laser intensities.

3.4. Measurement of the fluorescence intensity as a function of laser power

In figure 8 the dependence of the fluorescence intensity, and hence excited beam density, on the intensity of the incident laser radiation is depicted. The density of excited targets increases rapidly as laser intensity increases, tending towards a saturation limit as the laser intensity increases beyond 150 mW mm $^{-2}$. This characteristic shows that an increased number of atoms detuned away from line resonance within the Doppler profile are excited as the laser power increases. These results indicate that experiments requiring a maximum density of excited atoms in the interaction region (as in the (e,2e) experiments which are to be performed) also require high laser intensities to optimize the excited-state signal.

4. Conclusion

An atomic beam oven has been described which can operate at temperatures in excess of 750 °C for use with calcium and other targets. The oven has several advantages, including efficient operation and a design that allows the oven to be removed and re-installed in its housing without loss of alignment of the interaction volume. The atomic beam from the oven has been characterized using laser induced fluorescence, and the operating parameters where radiation trapping is minimized for maximum beam density have been determined. A detailed set of CAD drawings of the oven are available on the web page linked to this paper.

Acknowledgments

The authors are grateful to Professor K Ross for advice and for sharing his experience of calcium ovens. We would like to thank Dave Coleman at the Schuster Laboratory for excellent technical assistance and for machining of the oven. The financial support of the Engineering and Physical Science Research Council, UK, is gratefully acknowledged.

References

[1] Ross K J and Sontag B 1995 *Rev. Sci. Instrum.* **66** 4409
[2] Buckman S J, Gulley R J, Moghbelalhossein M and Bennett S J 1993 *Meas. Sci. Technol.* **4** 1143
[3] Giordmaine J A and Wang T C 1960 *J. Appl. Phys.* **31** 463
[4] Pejcev V, Ottley T W, Rassi D and Ross K J 1978 *J. Phys. B: At. Mol. Phys.* **11** 531
[5] Hamdy H, Beyer H J and Kleinpoppen H 1990 *J. Phys. B: At. Mol. Opt. Phys.* **23** 1671
[6] Chwirot S, Srivastava R, Dyl D and Dygdala R S 1996 *J. Phys. B: At. Mol. Opt. Phys.* **29** 5919
[7] Dyl D, Dziczek D, Piwinski M, Gradziel M, Srivastava R, Dygdala R S and Chwirot S 1999 *J. Phys. B: At. Mol. Opt. Phys.* **32** 837
[8] Feuerstein B, Zatsarinny O I and Mehlhorn W 2000 *J. Phys. B: At. Mol. Opt. Phys.* **33** 1237
[9] Law M R and Teubner P J O 1995 *J. Phys. B: At. Mol. Opt. Phys.* **28** 2257
[10] Bizau J M, Gerard P, Wuilleumier F J and Wendin G 1987 *Phys. Rev.* A **36** 1220
[11] Ueda K, West J B, Ross K J, Hamdy H, Beyer H J and Kleinpoppen H 1993 *Phys. Rev.* A **48** R863
[12] West J B, Ueda K, Kabachnik N M, Ross K J, Beyer H J and Kleinpoppen H 1996 *Phys. Rev.* A **53** R9
[13] Ueda K, West J B, Ross K J, Kabachnik N M, Beyer H J, Hamdy H and Kleinpoppen H 1997 *J. Phys. B: At. Mol. Opt. Phys.* **30** 2093
[14] Ueda K, Kabachnik N M, West J B, Ross K J, Beyer H J, Hamdy H and Kleinpoppen H 1998 *J. Phys. B: At. Mol. Opt. Phys.* **31** 4331
[15] Beyer H J, West J B, Ross K J and De Fanis A 2000 *J. Phys. B: At. Mol. Opt. Phys.* **33** L767
[16] McLaughlin K W, Afloatooni K and Duquette D W 1997 *Phys. Rev.* A **55** 3615
[17] Lellouch L P and Hunter L R 1987 *Phys. Rev.* A **36** 3490
[18] Beverini N, Giammanco F, Maccioni E, Strumia F and Vissani G 1989 *J. Opt. Soc. Am.* B **6** 2188
[19] Murray A J and Read F H 1993 *Phys. Rev.* A **47** 3724
[20] Thermocoax Bd Henri Sellier, F92156 Suresnes Cedex, France. http://www.thermocoax.com.
[21] Ross K 2001 private communication